FAA-74-15

REPORT NO. FAA-RD-74-149



# LIDAR SYSTEMS FOR MEASURING VISIBILITY
# A TECHNICAL ASSESSMENT

J. R. Lifsitz

SEPTEMBER 1974

FINAL REPORT



Prepared for

U.S. DEPARTMENT OF TRANSPORTATION

FEDERAL AVIATION ADMINISTRATION
Systems Research and Development Service
Washington DC 20591

**Technical Report Documentation Page**

| 1. Report No. | 2. Government Accession No. | 3. Recipient's Catalog No. |
|---|---|---|
| FAA-RD-74-149 | | |

| 4. Title and Subtitle | 5. Report Date |
|---|---|
| LIDAR SYSTEMS FOR MEASURING VISIBILITY<br>A TECHNICAL ASSESSMENT | September 1974 |
| | 6. Performing Organization Code |
| 7. Author(s) | 8. Performing Organization Report No. |
| J. R. Lifsitz | DOT-TSC-FAA-74-15 |
| 9. Performing Organization Name and Address | 10. Work Unit No. (TRAIS) |
| U.S. Department of Transportation<br>Transportation Systems Center<br>Kendall Square<br>Cambridge MA 02142 | R5101/FA415 |
| | 11. Contract or Grant No. |
| | 13. Type of Report and Period Covered |
| 12. Sponsoring Agency Name and Address | Final Report<br>July 1973 - March 1974 |
| U.S. Department of Transportation<br>Federal Aviation Administration<br>Systems Research and Development Service<br>Washington DC 20591 | 14. Sponsoring Agency Code |

15. Supplementary Notes

See also: Report No. FAA-RD-74-29, THE MEASUREMENT OF ATMOSPHERIC VISIBILITY WITH LIDAR: TSC FIELD TEST RESULTS Final Report, March 1974

16. Abstract

A study has been made of the feasibility of using a laser backscatter system (lidar) to measure slant visibility at airports. This report summarizes the present status of lidar from a technical standpoint. Based largely on the results of experimental lidar field tests reported previously, the report isolates essential factors which bear on decisions regarding further lidar development. The following elements, upon which the success of an operational lidar visibility system will hinge, are discussed in detail:

- Detector and receiver dynamic range
- Minimum and maximum range limits
- Signal processing (instant vs time-average)
- Interpretation of data
- Multiple scattering
- Eye safety criteria

While some of these can be dealt with in the process of hardware design, others (e.g., multiple scattering, data interpretation) will probably require extensive testing of an engineering prototype system to acquire a "feel" for their operational significance.

| 17. Key Words | 18. Distribution Statement |
|---|---|
| Lidar, Slant Visual Range,<br>Low Visibility Measurements | DOCUMENT IS AVAILABLE TO THE PUBLIC THROUGH THE NATIONAL TECHNICAL INFORMATION SERVICE, SPRINGFIELD, VIRGINIA 22151. |

| 19. Security Classif. (of this report) | 20. Security Classif. (of this page) | 21. No. of Pages | 22. Price |
|---|---|---|---|
| Unclassified | Unclassified | 68 | |

Form DOT F 1700.7 (8-72) Reproduction of completed page authorized

# PREFACE

This report presents a technical assessment of the status of the lidar technique as a potential means for measuring slant visibility near airports. Prepared in partial fulfillment of the requirements of PPA FA-415, the report completes a feasibility program performed for the FAA by the Optical Devices Group of the Transportation Systems Center. A preceding report (No. FAA-RD-74-29) presents results of the TSC Lidar field test program.

The author wishes to acknowledge the contribution of Mr. C.A. Douglas, who made a number of suggestions for enhancing the clarity and accuracy of the material presented.

# TABLE OF CONTENTS

TABLE OF CONTENTS (CONTINUED)

## LIST OF ILLUSTRATIONS

## LIST OF TABLES

## LIST OF SYMBOLS AND ABBREVIATIONS

| SYMBOL | DEFINITION |
|---|---|
| A | area of receiver objective |
| ADP | avalanche diode photodetector |
| ALCH | approach light contact height |
| ALS | approach light settings |
| B | bandwidth of detection electronics |
| c | speed of light |
| CW | continuous wave |
| D | point along glide slope at which decision height is reached |
| $E_c$ | corneal irradiance, $w\text{-}cm^{-2}$ |
| e | electronic charge |
| f(R) | geometrical overlap factof or lidar optics |
| f | pulse repetition frequency |
| h | energy optical photon |
| $I_D$ | detector dark current (cathode) |
| J | Joule |
| mrad | milliradian |
| n | no. of signal pulses averaged |
| $N_\lambda$ | spectral radiance, $w\text{-}m^{-2}\text{-}nm\text{-}sr^{-1}$ |
| nsec | nanosecond |
| NBS | National Bureau of Standards |
| P | optical power (radiant flux), watts |
| $P_B$ | optical power detected from background |
| PMT | photomultiplier tube |
| PRF | pulse repetition frequency |
| Q | lidar system parameter (See Equation 2-6) |
| R | range |
| $R_1$; $R_m$ | minimum working distance; maximum effective range, m |
| $\Delta R$ | range interval |
| RVR | runway visual range |
| S(R) | S-function (Equation 4-3) |

## LIST OF SYMBOLS AND ABBREVIATIONS (CONTINUED)

| SYMBOL | DEFINITION |
|---|---|
| sr | steradian |
| SVR | slant visual range |
| T | transmissivity |
| $t_b$ | transmittance over baseline b |
| TLV | threshold limit value of ocular exposure |
| $V_K$ | Koschmieder visibility |
| VGS | visual guidance segment |
| $\beta(R)$, Pb, $\beta$ | volume backscatter coefficient at range R, $m^{-1}$ |
| $\delta, \upsilon$ | angles |
| $\lambda$ | wavelength, nm |
| $\eta$ | quantum efficiency |
| $\Omega$ | solid angle, sr |
| $\sigma(R)$ | extinction coefficient at range R, $m^{-1}$ |
| $\overline{\sigma}$ | (spatially averaged extinction coefficient, $m^{-1}$ |
| $\Upsilon$ | pulse width of laser |

# 1. INTRODUCTION

## 1.1 THE NEED FOR NEW TECHNIQUES TO MEASURE VISIBILITY

If aircraft landings are to be carried out routinely under CAT II (and eventually CAT III) conditions,* new methods and systems for measuring visibility must be developed. Slant visibility, a measure of the pilot's ability to see ground cues during the final stages of approach, demands particular attention.

The FAA, as well as the Air Force and Navy, has for the past several years supported studies to examine and assess alternatives for determining slant visibility. Among these is the use of the lidar method (optical backscattering). This report assesses lidar, apparently the most promising alternative, in the light of the findings of a number of such studies.

Presently, the only system in general use to measure visibility at airports is the NBS/FAA AN/GMQ-10 transmissometer, developed in the 1940's for runway visual range (RVR). While this system can give useful information about ground visibility, it does not provide a basis for the measurement of approach visibility. In a low visibility landing, the time between visual cue acquisition and touchdown is critically short. A pilot needs to know whether, or not, at decision height and below, as he moves along the glide path, these cues will be visible. The transmissometer is not a suitable source of such information for several reasons.

First, RVR readings taken along the runway yield little information about conditions in the approach zone, which is over half a mile away. Airport approaches are often over water, or

*CAT II: Condition of aircraft operations permitting landings at runway visual range down to 1200 feet, with the decision whether to land being made at 100 foot altitude.

CAT III: RVR>700 ft (IIIA), no decision height specified.

over land whose surface characteristics differ significantly from the flat concrete and asphalt areas of the runways. This can lead to wind and temperature gradients and consequently to visibility conditions showing marked horizontal variation. Moreover, even where it is possible to put a conventional transmissometer on the ground, but within the approach region, lack of information on possible vertical gradients again renders its use questionable. To directly assess the slant situation with a transmissometer, the receiver would have to be at least 100 feet in the air, mounted on a rugged tower. Clearly, this is impractical and potentially dangerous.

Several novel approaches were taken to the problem in the '60s, each of which was based on the scattering of light from fog or clouds. In most cases, the instrument consists of a ground-based optical transmitter and receiver, arranged so that the receiver field-of-view intercepts the transmitted beam in a limited volume of space. This volume can be made to fall along the glide slope, for example.

The total amount of scattered light received at the detector, in such cases, depends on two characteristics of the atmosphere:

1. The strength of scattering from the intercept volume into the direction of the receiver and within its field-of-view, and
2. The total attenuation of the light due to the intervening aerosol.

The scattering from the common volume is generally observed at 180° to the direction along which the light is transmitted.

Visibility over a given path is related to the extinction over that path, as discussed below. Extinction in fog and clouds is usually assumed to be due to scattering only, since water droplets absorb negligibly at most visible and IR wavelengths.

Instruments which measure total energy backscattered from a common volume have the following limitations:

1. Their calibration assumes a constancy in the ratio of angular scattering coefficient to the extinction coefficient. The assumption is not, in general, a good one, since this ratio depends on the distribution of sizes as well as the refractive indices and shapes of the particles involved in the scattering. (In some situations, especially on the east coast of the United States, where poor visibility is often caused by characteristically uniform fog, a total energy backscatter device, such as the "Videograph" made by Impulsephysik, has had some success).[1]

2. They are generally insensitive to the presence of inhomogeneous conditions. Even simple patterns, such as a low ceiling, cannot be detected by most of these systems. Incomplete information about overall conditions can be dangerously misleading.

It was to overcome deficiencies such as these that attention turned to time-resolved lidar("light detection and ranging") techniques.

## 1.2 THE LIDAR TECHNIQUE

Lidar differs from the optical methods discussed above in that it has the capacity for ranging. To this end, lasers are usually used for the transmitter source; these offer short intense optical pulses (10-100) nsec) and high spectral radiance.*

"Lidar" will be used here to mean specifically a technique which analyzes the temporal dependence (or signature) of the received pulse of radiation. This distinguishes, for example, a

*Modulated CW sources have also been discussed for lidar use.[2] However, they have no particular advantages over pulsed systems, nor have they been used successfully in measurements of visibility. We only consider pulsed sources in this report.

lidar from a laser ceilometer. Ideally, a lidar visibility system would measure the distribution of atmospheric extinction in space and relate this information to visibility over a given range.

### 1.2.1 Progress in Visibility-related Lidar Work

In 1967, Brown[3] showed that a correlation exists between shape parameters (width, distance-to-peak) of a backscattered lidar signature and the atmospheric extinction coefficient. His analysis of the signature led to a measurement of extinction without explicit knowledge of the ratio between extinction and backscatter coefficients.

The parameters chosen to characterize the signature relate to Brown's use of a bistatic lidar, with transmitter and receiver separated by up to a few feet. This required careful alignment of the two, making accuracy difficult to achieve and maintain. Furthermore, in low visibility, the signature width and distance-to-peak are rather insensitive to variations in extinction.

Subsequent efforts[4,5,6,7,8] have instead analyzed the shape factor most characteristic of extinction effects, namely the exponential falloff of intensity with range. This approach is more sensitive to extinction, adds the potential for range resolution, reduces sensitivity to optical alignment, and permits the use of a coaxial transmitter-receiver configuration.

While most of the analysis has dealt with relatively homogeneous conditions, some, notably by Collis and co-workers,[4,5,7] has been applied to the much more complex problem of measuring non-uniform visibility. More will be said of this problem in Section 5. Its potential ability to monitor visibility conditions such as these gives lidar an advantage over all other methods; it also presents the lidar system designer with his greatest challenge.

## 1.3 SLANT VISIBILITY CONCEPTS

Figure 1 shows the geometry of the approach situation, including the 3° glide slope, decision heights at 100 and 200 feet, and bars of approach lights, spaced at 100 foot intervals and extending out from the threshold.

There are a number of ways to describe approach visibility, although a final operational definition has not yet been established by the FAA. Several commonly used terms are:

Slant Visual Range (SVR): A "working" definition of SVR is as follows[10]: "SVR is the slant distance to the farthest high intensity runway edge light or approach light which a pilot will see at an altitude of 100 feet on the approach path or, if large, the slant distance which would have a transmittance of 5.5%." Referring to Fig.1, the line AB would correspond to the SVR.

Visual Guidance Segment (VGS): A related concept is the visual guidance segment which is the "length of a segment of approach lights (expressed as a distance in hundreds of feet) which a pilot will see at an altitude of 100 feet on the approach path without regard to cockpit cutoff angle."[9] This concept is called the "slant visual range" in Reference 9 but "visual guidance segment" is more descriptive of its meaning. Referring to Fig. 1, segment AD would be the VGS corresponding, under either uniform or vertically-layered visibility conditions, to the SVR (AB). In this case, the numerical values of the SVR and VGS are approximately the same, as can bee seen from the geometry. For example, if the SVR is 600 feet, the VGS differs from it by less than 2%. (One can readily conceive of fog distributions, however, for which the values of the two quantities are very different.)

Approach Light Contact Height(ALCH): The height at which a pilot will see and should continue to see a minimum of five light bars of approach lights at 100 foot spacings, if extended to touchdown. (This assumes the approach lights are extended indefinitely at the same spacing and intensity). A standard cockpit cutoff angle of 15 degrees shall apply."[9]

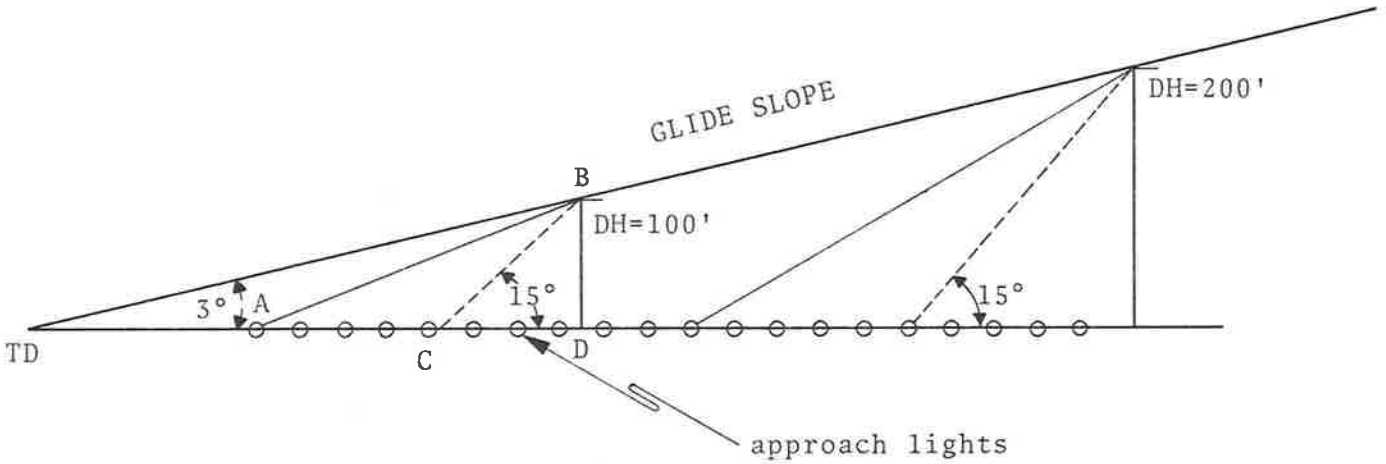


Figure 1. Geometry of Approach Zone, Showing SVR as Defined in Ref. 9

Whatever the final operational definition of "approach visibility", it need not concern us here. In general, for the present purpose, approach visibility or slant visibility will measure the ability of a pilot, at decision height, to see the references on which he relies for a confident descent and landing.

In order to acquire this confidence, the pilot must see some minimum number of lights or bars to establish a useful pattern. One common criterion is that at least five light bars should be visible at decision height, taking into account the 15° cutoff angle of the cockpit. The "five light" criterion implies a minimum critical path over which the pilot must see at decision height (DH). The critical path (or minimum operating SVR) will be discussed in Section 2.

At times in this report, "visibility" will mean the meteorological range or Koschmieder visibility, $V_K$, based on contrast. Intitial target contrast is taken as unity, and the liminal value of .02 is used. The use of this visibility often simplifies the discussion when value of extinction coefficient ($\sigma$) are involved. By the well known Koschmieder relation, $V_K = 3.91/\sigma$, the extinction measurements can be readily related to visibility.

The liminal contrast used in the United States is .055, while the World Meteorological Organization uses .05. To convert from the meteorological range used in this report to the common operational visibility, one must multiply $V_K$ by .75.

# 2. LIDAR PROBING RANGE

The distance interval over which lidar can be useful is limited on the low end primarily by geometrical considerations and, at the high end, by signal-to-noise criteria.

## 2.1 MINIMUM RANGE

The usefulness of the lidar is limited in the near field primarily by geometric optics. Whether a coaxial or bistatic arrangement is used, the limitation will be effectively the same. In the immediate vicinity of the lidar, no backscattering can reach the detector. This is due to the absence of beam overlap, for bistatic systems, and to obscuration by beam-steering optics, in coaxial configurations.

Thus near-field effects produce a "dead-zone" between the lidar and a minimum range $R_1$, within which extinction measurements cannot be made. To some extent there is a trade-off between beam spread and $R_1$. However, the criteria for selecting beam spread include more than a concern for minimizing $R_1$. For example, large beam divergence (>several mrad) may lead to severe contributions from mutiple scattering. On the other hand, too tight a receiver field of view may not provide sufficient representation of the atmosphere along the direction sampled. In addition, the beam divergence will be dictated in part by the source configuration and characteristics. Thus, high power diode laser arrays cannot be collimated to better than about 6 mrad (full angle) whereas ruby or erbium beams can be reduced to a fraction of a milliradian. It appears that a practical value for $R_1$ is around 30-40 meters.[6,7]

## 2.2 MAXIMUM RANGE

The maximum range $R_m$ over which lidar gives useful information is fundamentally limited by the noise accompanying the backscattered signal. During daylight hours, noise arises from fluctuations in photocurrent due to background radiation and from intrinsic detector noise. At night, the intrinsic noise of the detection system is dominant.

One must provide sufficient dynamic range of detection to fully exploit the available signal. Receiver dynamic range is primarily a technical problem (see Section 3), and is not a fundamental limit to a practical lidar system. We assume below that this problem has been (or can be) solved satisfactorily and only consider noise limitations on $R_m$.

An expression for $R_m$ can be found by combining the lidar equation with the equations representing noise. The lidar equation, giving the radiant flux, P(R), of the optical signal received from the region of space at distance R, under homogeneous atmospheric conditions, is

$$P(R) = \frac{P_o A \beta_b e^{-2\sigma R}}{R^2} \frac{(c\tau/2) f(R)}{} \qquad (2\text{-}1)$$

where $P_o$ = peak radiant flux of lidar output pulse

$A$ = receiver objective area

$\beta_b$ = volume backscatter coefficient*

$\sigma$ = extinction coefficient

$\tau$ = outgoing pulse width

$c$ = speed of light

$f(R)$ = geometrical factor for receiver overlap

* The subscript will be dropped for the remainder of this report since scattering in the backward direction only is of interest here.

It should be recognized that Equation 2-1 is based on single scattering theory. Without the single scattering idealization, it is virtually impossible to discuss the lidar signature quantitatively and in closed form. Higher order scattering contributions, discussed in Appendix B, are difficult to estimate and will require empirical treatment.[7]

Since we are interested in relatively large distances $R_m$, the receiver and transmitter fields-of-view are assumed to be completely overlapped [$f(R) \rightarrow 1$]. The backscatter coefficient $\beta$ is not uniquely related to the extinction coefficient $\sigma$. For the present calculation, an empirical relationship found to hold in stratus clouds[12] will be used. This gives:

$$\beta = \frac{0.6\ \sigma}{4\pi} \quad .$$

So far we have dealt in terms of extinction coefficient, though it might seem that "visibility" would be more useful. However, the conversion from extinction to visibility depends on the type of visibility meant. Lidar measurements can be applied to situations involving either contrast (of objects or markings) where Koschmieder's equation is used, or the perceptibility of approach lights. In either case the visibility is a function of more than just the extinction coefficient. Such factors as background luminance, approach light intensity and scattering from external sources into the eye of the observer, all affect the visibility.[11]

The introduction of these additional parameters would obscure the clarity of the present derivation. Once $R_m$ is found as a function of $\sigma$, its dependence on a specific kind of "visibility" can be found from an appropriate nomograph.

The detected background radiant flux $P_B$ is given by

$$P_B = N_\lambda \Delta\lambda \Omega\ A\ T_o, \qquad (2\text{-}2)$$

where $N_\lambda$ = spectral radiance of background, w-m$^{-2}$-nm$^{-1}$-sr$^{-1}$

$\Delta\lambda$ = spectral bandpass of receiver, nm

$\Omega$ = solid angle of receiver field-of-view, sr

$T_o$ = overall transmission of receiver optical elements.

An expression for the ratio of signal voltage to rms noise (S/N), averaged over n signal pulses, is

$$S/N(R) = \left(\frac{\eta}{h\nu}\right)\left(\frac{ne}{2B}\right)^{1/2} \frac{P(R)}{\left[\frac{ne}{h\nu}\ [P(R) + P_B] + I_D\right]^{1/2}} \qquad (2\text{-}3)$$

where $\eta$ = detector quantum efficiency

$B$ = detection electrical bandwidth $\simeq \frac{1}{2\tau}$

$h\nu$ = energy of laser photons = 2.3 X $10^{-19}$ J at $\lambda$ = 900 nm

$e$ = electronic charge = 1.6 X $10^{-19}$ coul

$I_D$ = detector dark current

Equation (2-3) holds when the internal gain of the detector (e.g., PMT) is large enough to overcome the thermal noise.* The noise included in the expression is shot noise due to fluctuation in photoelectron current arising from signal photons, background photons and dark current, respectively. The relative importance of these terms will clearly depend on the system and background conditions under consideration.

The minimum acceptable ratio for S/N ($R_m$) is selected to be 10. (It is not sufficient that the signal from range $R_m$ be just detectable. Its amplitude must be measured accurately enough to deduce the extinction coefficient.)

*See, for example, reference 13, p. 177. Note that Equation (10-11) of that reference is in terms of power ratios, whereas Equation (2-3) above has been revised to a voltage ratio which is more relevant to the lidar detection.

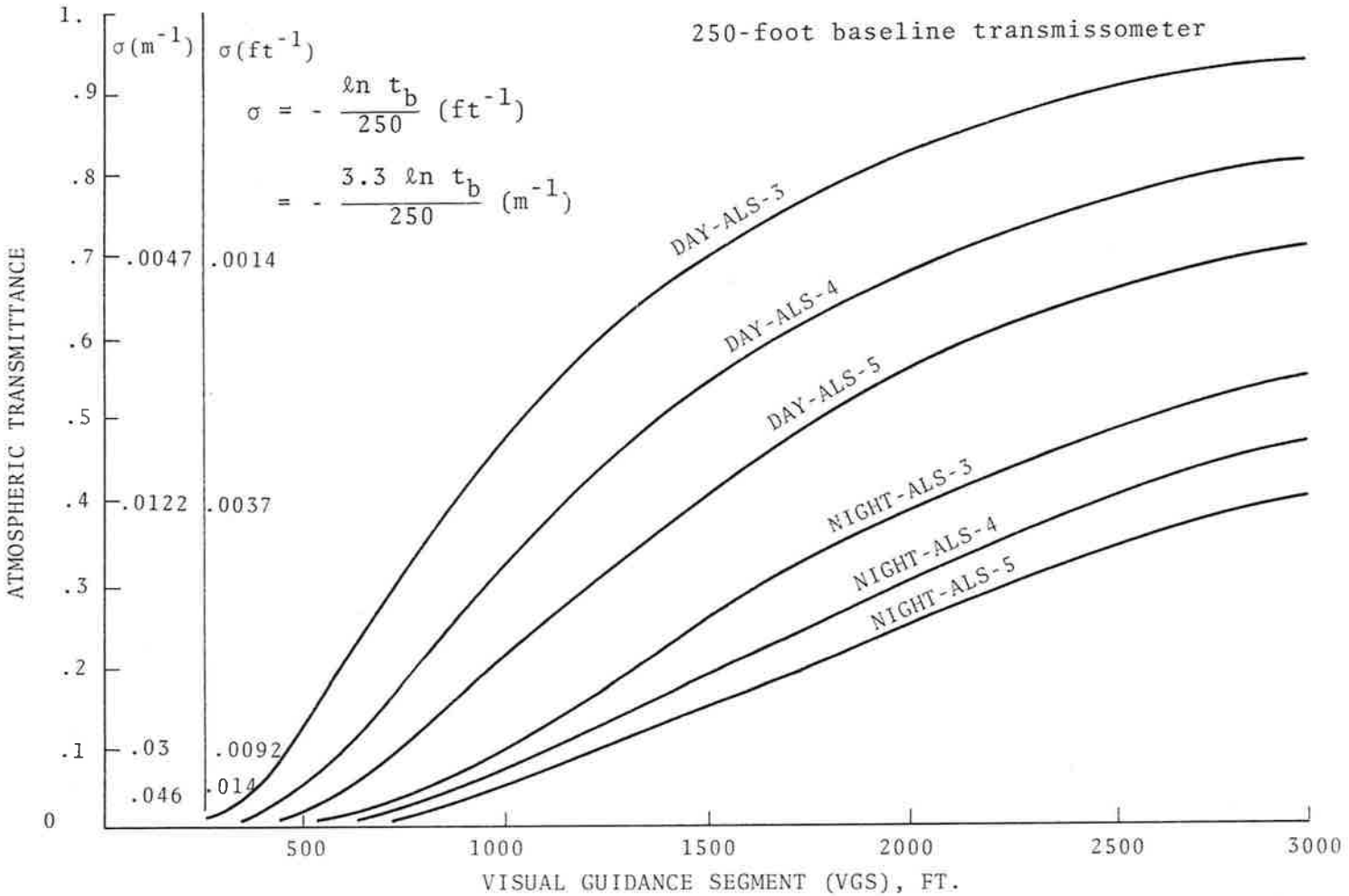


Figure 3. Visual Guidance Segment (VGS) from 100-ft Versus Atmospheric Transmittance $t_b$ for Three Approach Light Settings and the Day and Night Illuminance Threshold.

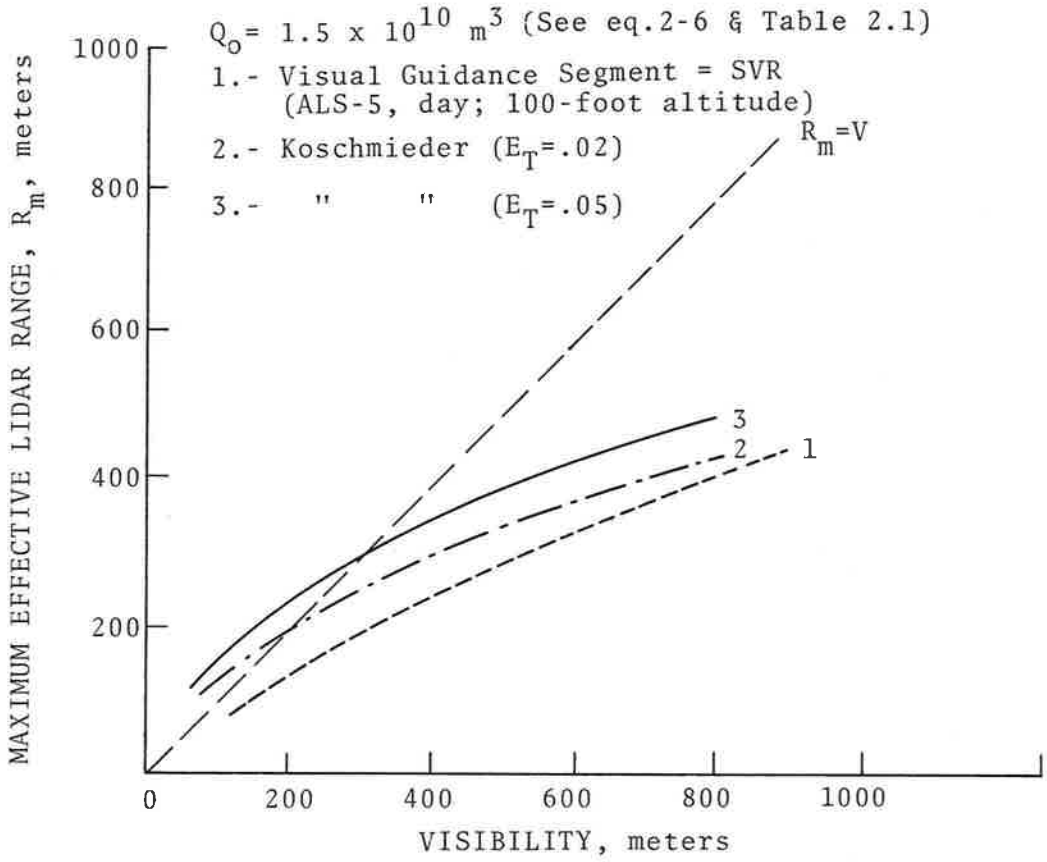


Figure 4. Maximum Effective Lidar Range, $R_m$, Versus Visibility for $Q_o$= 1.5 x $10^{10}$ $m^3$ and Three Differently Defined "Visibilities". The Line $R_m$ = V is drawn for Comparison.

be approximately $R_m = V/4$.

Figure 4 can be used to infer something about the operational use of lidar. Assume, for example, that the pilot, to descend below the 100 ft decision height, must be able to see a minimum of five light bars beyond the 15° cockpit cutoff angle. Then, referring to Figure 1, the minimum acceptable SVR is approximately the length of segment AB, or 260 meters. However, as we have seen with respect to approach lights at intensity setting 5, the lidar range $R_m$ would be one-half the visibility, at best. Therefore, to obtain data from the region of space near the decision height, the lidar must be placed somewhere near point C (Figure 1), directed upward toward point B.

# 3. DYNAMIC RANGE

## 3.1 REQUIREMENTS

Dynamic range relates in two ways to lidar signal detection. First, the receiver must be able to handle the range of peak signal amplitudes corresponding to the variation in extinction coefficient which the system will encounter. Second, and more of a challenge, the receiver has to deal with the extreme range of signal amplitudes that occurs for any given signature. This amplitude range extends from approximately the signal peak to the value at distance $R_m$ (Section 2). See Figure 5.

The first of these problems can be handled with relative ease, since the distribution of extinction coefficient changes slowly with time. Detector gains can be altered to take account of the changing signal peak value.

On the other hand, the dynamic range across the signature envelope, arising partly from the $R^{-2}$ decrease in signal and, more significantly in low visibility, from the two-way exponential attenuation with distance, is more difficult to handle. The signal, from its peak to the value at $R_m$, can span four decades or more (80 dB)*, as seen in Figure 6. The value of $R_m$ marked on the curves corresponds to the results of Section 2; visibilities of 40 to 400 m are considered. It is this second case, the "relative" dynamic range, that is of concern in this section.

As seen in Figure 5, the minimum useful value of R ($R_1$) is just beyond the value of R corresponding to peak signal. The smaller values for $R_1$, and hence larger dynamic ranges, generally occur with poorer visibility, closer transmitter-receiver beam overlap and shorter transmitted pulses.

*We will use the following decibel notation throughout: No. of dB = $20 \log\left[\frac{V_2}{V_1}\right] = 20 \log \frac{i_2}{i_1}$, where V and i are signal voltage and detector current, respectively.

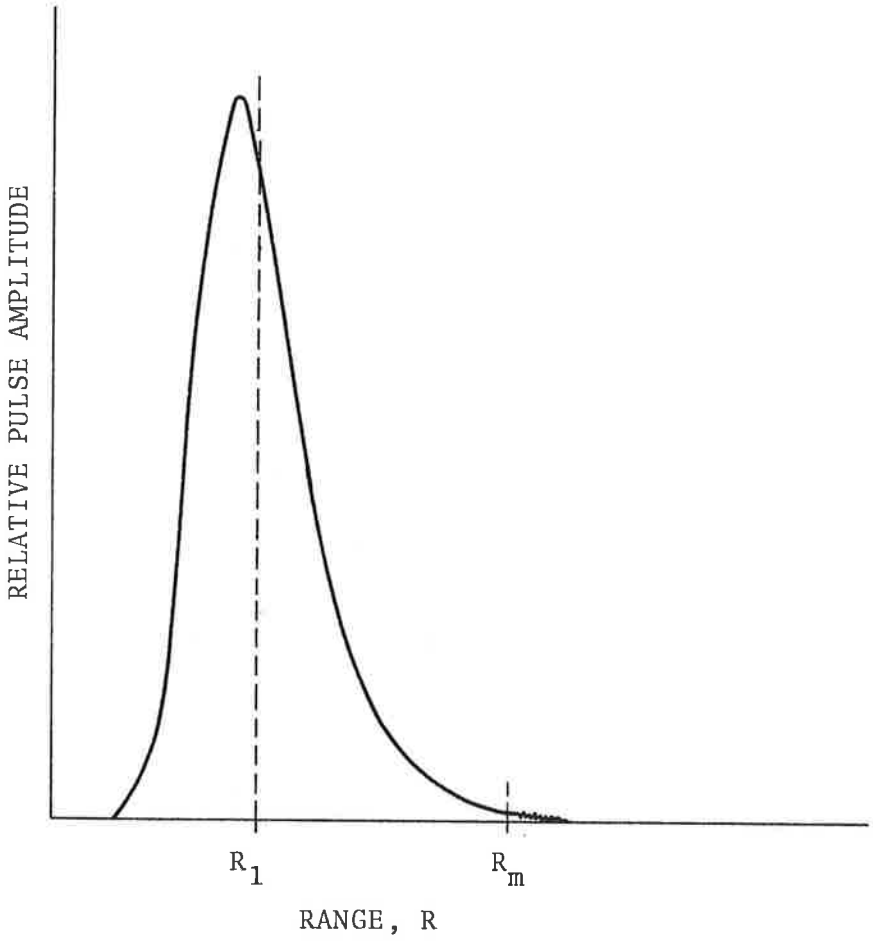


Figure 5. Ideal Lidar Signal Shape, Showing Positions of Minimum and Maximum Ranges $R_1$, $R_m$

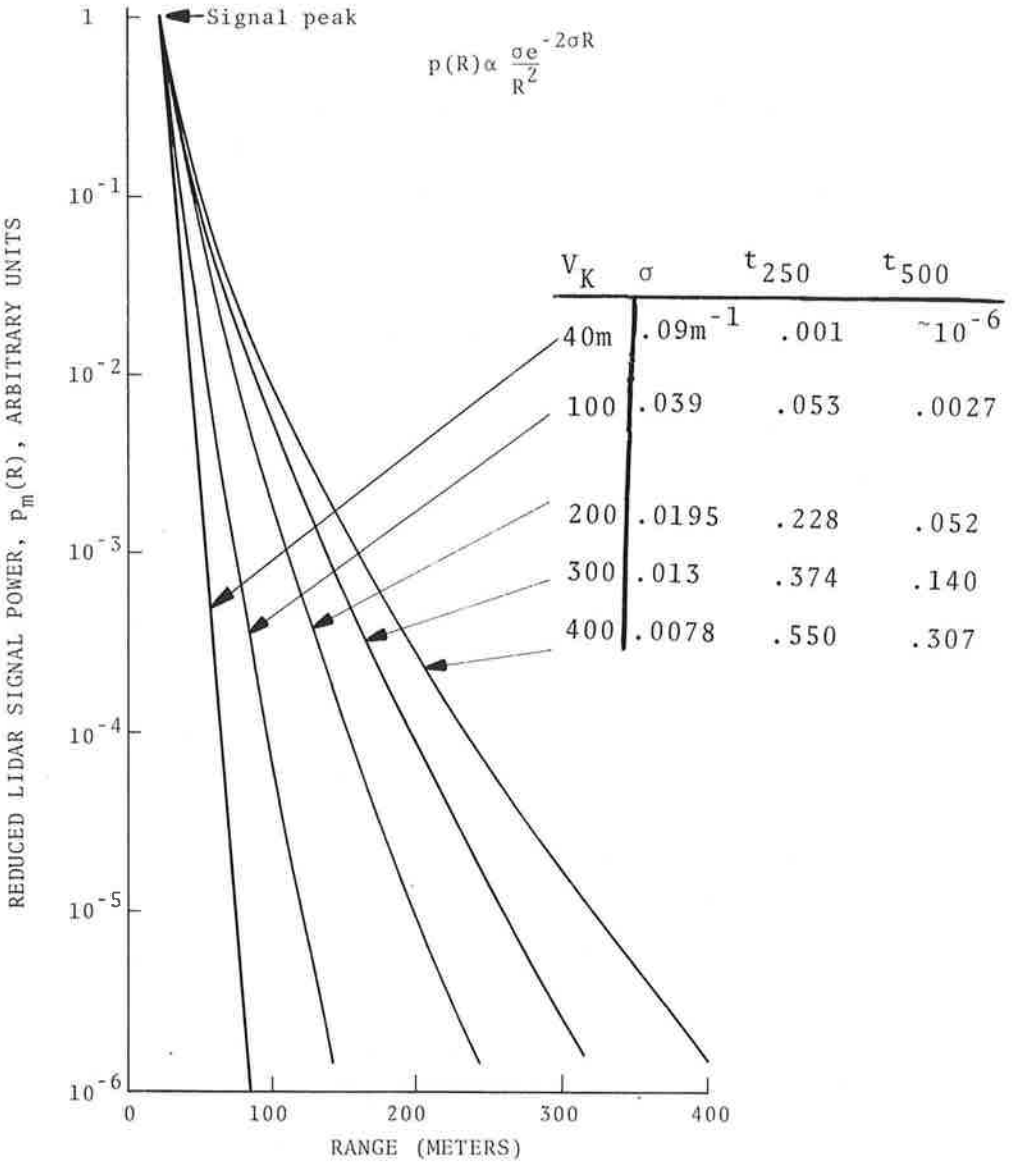


Figure 6. (Reduced) Lidar Signal Versus Range, for Several Values of Visibility $V_K$ and Extinction Coefficient

## 3.2 IMPLICATIONS FOR RECEIVER SYSTEMS

The receiving system includes, in addition to the optics, the detector and its power supply and the succeeding amplification electronics. The large dynamic range will have implications for both the detector and the electronics which follow it.

### 3.2.1 Detectors

The two types of detectors which have been used in experimental lidar systems are the photomultiplier tube (PMT) and the avalanche photodiode (ADP). The requirements for any lidar detector are that:

1. the instantaneous photocurrent i(t) must be a linear function (or a well calibrated and stable non-linear function) of the instantaneous optical power on the detector surface;
2. the photosignals, for the range of optical intensities encountered, must be sufficient to dominate amplifier noise;
3. the device must not be damaged by the level of photocurrent drawn.

Generally, accurate representation of lidar signatures requires electronic bandwidths of about 30 MHz and corresponding load resistance of 100 ohms or so. Assuming that the effective input noise of the wideband amplifier following the detector is 100 μV and that a minimum signal to noise ratio of 10 is desired at the maximum lidar range $R_m$, then the instantaneous photocurrent $i\left(t = \frac{2R_m}{c}\right)$ corresponding to the signal from $R = R_m$, must be approximately 10 μA. Signal averaging techniques will reduce the required minimum currents to perhaps as low as 1 μA.

As shown in Figure 6, the signal originating from $R_1$, near the peak of the pulse, may be ten thousand times the minimum. The resulting peak currents, 10 to 100 mA, are close to the tolerable limit for linear PMT response (especially for tubes with an S-20 or extended-red response needed in the near IR.

A test of a silicon ADP in our laboratory has shown the non-linearity sets in for photocurrents above 1 mA. (One manufacturer agreed that this may be a typical upper limit, due to carrier depletion). For its part, on the other hand, the ADP has a 50% or greater quantum efficiency, almost an order of magnitude better than any of the photocathodes available for near infrared wavelengths. As shown in Section 2, this is advantageous when measurements are limited by noise due to background radiation.

One way to meet the dynamic range problem is to restrict the part of the signature analyzed to the amplitude range over which linearity has been demonstrated. However, this reduces the volume over which the lidar is useful. Also, peak signals may be somewhat higher than the signal at $R_1$; one must be wary of detector overload and ensure that recovery is fast enough to stabilize the detector gain by the time $t = \frac{2R_1}{c}$.

Several points should be considered regarding requirements of PMT's, though not directly related to the problems of relative dynamic range.

1. The tube should be gated on and off, just before and just after the lidar signal is present at the detector. The average photocurrent due to background sources is thereby greatly reduced, preventing both spurious gain behavior and accidental damage to the tube.

2. The PMT biasing chain must be designated to handle fast pulses of light without depletion of dynode potentials (and hence non-linearity in the gain). Capacitive bypassing of the final stages of the dynode chain, as well as Zener diode stabilization of the cathode - 1st dynode potential, are commonly used.

3. The range of absolute peak signal values can be met, for example, by measuring the peak value with a relatively insensitive detector and adjusting the PMT gain.

### 3.2.2 Receiver Electronics

The transfer function of an electronic amplifier generally has a linear range limited to about 40 dB, or an input amplitude span of 100:1. Even if it were possible to obtain linear amplification over a much larger range, there would still remain the problem of storing signals usefully. Analog storage devices generally operate over less than two decades while a 10-bit digital sampling unit has a maximum dynamic range of about 60 dB. It would appear that, without some sort of time variation of the amplifier gain, presumably over the duration of the return pulse, the lidar signature cannot be optimally exploited.

## 3.3 ACQUISITION: "BOXCAR" VS. TRANSIENT RECORDER

Assuming for the moment that a method of detection having suitable dynamic range of linearity is available, we will consider two basic ways of acquiring signals. These approaches are commonly referred to as: 1) the "boxcar" and, 2) the transient recorder, the names suggesting the underlying principles of widely used devices.

This topic is introduced here, rather than under "signal processing" since the choice of acquisition scheme may restrict, or be restricted by, the methods available for compressing dynamic range, largely because of bandwidth considerations.

### 3.3.1 "Boxcar" Method (Slow Range Sweep)

The boxcar technique is commonly used for extracting repetitive signals from noise. Since the signal is usually assumed to be identical for each cycle, it lends itself to slow sweep acquistion processes, with a narrow range gate sampling a small part of the signal at any instant. A large number of pulses can in this way be averaged at any range R, the number depending both on the range sweep rate and on the pulse repetiotion rate. If the noise accompanying each pulse is random, the average noise tens toward zerol With the completion of one sweep, the signal is reconstructed with an enhanced signal-to-noise ratio.

Among commercial instruments which employ the boxcar principle, gate widths of 10 nsec are common. Experience[6,8] indicates that, using GaAs or GaAlAs laser sources with peak powers of several hundred watts and pulse repetition frequencies of 0.5 - 1 kHz, sweep durations of 20 seconds to one minute may be needed.

### 3.3.2 Transient Recorder

The transient recorder, as its name suggests, records a single pulse in its entirety. Triggered simultaneously with the output of the lidar transmitter, the recorder sweeps in real time, acquiring in discrete sampling channels (words) the instantaneous signal values. These analog-to-digital channels can be quite narrow in time; they afford good amplitude resolution as well. As an example, the Biomation 8100 transient recorder has 2000 8-bit words and gives 10 nsec time resolution with 0.4% amplitude resolution (dynamic range ~48 dB). Improvement in dynamic range is possible but at the expense of bandwidth. Thus, 10-bit resolution (dynamic range~60 dB) may mean minimum time resolution of 30-40 nsec.

The distinguishing feature of this technique, then, is that all the data in each return pulse is temporarily stored and immediately available for readout, in either digital or analog form. Methods to be used for readout and handling of the data will be the subject of discussion in Section 4.

The relative advantages of the boxcar and transient recorder method, a comparison which hinges largely on the updating and averaging requirements of the operational SVR system, will be discussed in Section 5. At this point, it is the type of hardware underlying these methods ["slow" electronics for boxcar, "fast" (wideband) for transient recorder] which is important, since this will play a role in the selection of signal compression techniques.

## 3.4 APPROACHES TO SIGNAL COMPRESSION

A number of methods for signal compression exist; they differ in accuracy, bandwidth and dynamic range capability. Of those mentioned here, some methods have been tried in experimental lidar systems. Others are more speculative in this application.

Operational Amplifiers

Perhaps the most efficient way to compress the detected lidar signal is to use a logarithmic amplifier (logamp). This not only compresses the range of amplitudes; a good portion of data reduction is accomplished at the same time. The reason for this can be seen by examining Equation 2-1. By writing the equation as

$$P(R) = \frac{Ke^{-2\sigma R}}{R^2} \qquad (3\text{-}1)$$

with K = constant (assuming the backscatter coefficient is independent of R), we have

$$-\frac{1}{2}\ \frac{d\ell n}{dR}\ (PR^2) = \sigma \qquad (3\text{-}2)$$

From equation 3-2 we see that, in relatively homogeneous atmospheric conditions, two measurements of log P yield the extinction coefficient. (See Section 4.2.1).

At Stanford Reasearch Institute (SRI), wideband logamps have been used with some success in lidar receivers.[5,7] Bandwidth is a crucial factor in logamp design because, since the amplifier has a non-linear input impedance (e.g., a diode), its reactive characteristics can depend on the signal amplitude. This gives rise to an amplitude-dependent bandwidth which, as reported by Viezee, et. al.[5], can distort the output.

Oblanas, et. al., [16] have recently developed an improved logrithmic amplifier, with 30 Mhz bandwidth and with accurate compression of almost 60 dB (1mV-1 volt output). In their lidar processing scheme, a signal proportional to 2($\ell$nR) is also generated and added to log P(R). When displayed on a linear range (time) scale, the resulting output ($\alpha\ell nR^2P$) is, if the atmosphere is homogenous, a straight line; the slope gives the extinction coefficient $\sigma$ directly (equation 3-2). Range resolution, according to the authors, is 10 meters.

It would seem that, in the slow scanning or "boxcar" mode, the logamp technique should be even more useful, with a possibility of 80-100 dB compression. The use of such an approach in lidar has not yet been reported.

Brown[6] has used range-squared correction, in a "boxcar" acquisition mode, to compensate for the $R^{-2}$ falloff in signal. He does not discuss the problem of dynamic range; $R^2$ compensation appears to be sufficient in his examples. This is probably due to the relatively long duration pulse width (80 ns) used and the realm of extinction studied (visibility>300 meters). Had his pulse width been as short as, say 30 nsec (desirable for improved resolution and to eliminate the need for deconvolving the source pulse from the backscatter signature),[8] and had he worked with visibilities under 300 meters, dynamic range might have caused more concern. Still, his results do indicate the range-squared compensation helps toward solving the compression problem.

Gain Switching

Switching the gain of a linear amplifier by known amounts, at certain points during the lidar range sweep, might be attempted. The problems with such an approach are several:

1. it is difficult to apply on a fast response basis;
2. the gains must be carefully calibrated and held very stable; and
3. it is improbable that a unique set of switching points and gain levels can be found which are applicable to all lidar signals.

Time Programmed Detector Gain

Allen and Evans[17] have used time programming of the overall detector(PMT) gain to compensate for the $1/R^2$ signal variation in real time. This is accomplished by applying a modulating voltage to several dynodes simultaneously. Over a gain range of 10:1, the control characteristics for each dynode pair is "relatively linear" to decibels of gain vs moduelating voltage. By applying the same waveform to

several stage pairs, a cumulative effect is produced; accurate $1/R^2$ signal compensation over 43 dB was obtained with this technique, over a total interval of about 7.5 km (50 μsec round trip delay).

Detector gating, whose accuracy requirements are less demanding than those of gain programming, may be used to limit the dynamic range burden of both the detector and the following amplifiers. The gain of the detector (e.g., PMT) is held at zero until a suitable time after the peak of the lidar signal has arrived. By applying step voltages to one or more of the dynodes, the gain is suddenly increased to its operating value. Gating with nanosecond switching times, as reported in the literature,[26,27] usually causes a subsequent "ringing" that can introduce serious inaccuracies in the signal shape measurement.

Recently, gating has been applied to a side-window PMT with gate widths as short as 12 ns, without the appearance of "ringing".[18] With short gates such as these, the on-time "window" of the PMT can be scanned across the lidar signal, in a boxcar mode of operation. The combination of this method with the range-squared compensation of the photocurrent, may lead to a satisfactory method for handling dynamic range.

Multiple Detectors

Less elegant than gating, but perhaps more straightforward, would be the use of a pair of detectors (one with high, the other with low sensitivity) arranged in a common receiver. By appropriate sampling the signature could be divided, say at mid-range, into manageable portions of approximately equal excursion in amplitude. The ratio of responsivities of the two detectors must be accurately known. Some gating, though not as sophisticated as that discussed above, may still be needed to minimize saturation effects in the high sensitivity detector.

Reduced Performance Options

If the methods mentioned above prove to be expensive or unusually complex, a simpler solution might be to reduce the total sampling interval, thereby reducing the span of signal amplitudes to perhaps 40-60 dB.

For example, a relatively useful device would result even if the dynamic range were reduced artificially, either by adjusting the optics and beam divergence for farther overlaps (larger $R_1$), or by discarding information beyond some cutoff distance $R<R_m$. Figure 6 shows that, for $V_K$ = 200m one might use only that portion of the lidar signature between 50m and 150m, giving a manageable dynamic range of 55 dB. This option must be weighed, of course, against the reduction in probing length along the critical path.

In conclusion, several methods have been suggested here for handling the large dynamic range which confronts the lidar designer. While it is worthwhile to exploit the full range of the lidar signature if possible, some compromise in dynamic range capability, to reduce system cost and complexity, may still allow adequate performance.

# 4. SIGNAL PROCESSING

## 4.1 THE PROCESS DEFINED

The phrase "signal processing" means here the procedure by which the lidar signal is converted from a time-dependent photocurrent to a stored representation of the backscatter signature (i.e., to data).

The choice of final form to which the signal is to be processed will depend on the method used for data interpretation. For example, if analog signal averaging is used, the final form of the signal processing will be the set of values of averaged signal versus range. On the other hand, when individual signatures are stored digitally and output in a "handshake" transfer to the buffer of a minicomputer, signal processing is complete before the transfer interface. Further treatment of the data in the computer will be considered "interpretation".

A previous discussion (Section 3.3) showed how processing may begin with the analog treatment of the detector photocurrent (e.g., logarithmic amplification). The first stage of signal processing will likely be determined by the particular method chosen to compress dynamic range.

The division of function into "signal processing" and "data interpretation" is admittedly arbitrary and not always possible. Nevertheless, such a distinction may be useful, particularly if a modular approach is taken to the development of the system.

## 4.2 METHODS OF DATA ANALYSIS

Two methods used for deducing extinction coefficient from optical backscatter signatures are the "ratio" and "slope" methods. Though they give similar results for homogeneous atmospheric conditions, the two approaches treat inhomogeneities quite differently. In addition, each technique is suited to a different form of signal processing.

4.2.1 "Ratio" Method

Of the two methods, the ratio method[6] gives a finer measure of the spatial variation of the signal. Signal amplitudes are compared at pairs of points relatively close to each other (close enough that the volume backscatter coefficient $\beta$ can be taken as the same for both points). The range coordinate axis is divided into intervals $\Delta R_i$. In practice, these are about 5 to 15 meters wide.

The lidar equation (2-1) can be used to find an expression for the average extinction coefficient $\sigma$ over interval i:

$$\sigma_i = \frac{1}{2\Delta R_i} \ln \left[ M_i \frac{\beta(R_{i+1})}{\beta(R_i)} \right] \qquad (4\text{-}1)$$

where

$$\Delta R_i \equiv R_{i+1} - R_i, \text{ and } M \equiv \frac{R_i^2 P(R_i) f(R_{i+1})}{R_{i+1}^2 P(R_{i+1}) f(R_i)} .$$

If the intervals $\Delta R_i$ are small enough, the variation in $\beta$ between end points can be ignored, leading to the useful approximation:

$$\sigma_i = \frac{1}{2\Delta R_i} \ln M_i . \qquad (4\text{-}2)$$

The average visibility between two widely separated points A, B is then obtained from the averaged extinction coefficient $\bar{\sigma}$; e.g., using the Koschmieder relation,

$$V_{AB} = \frac{3.91}{\bar{\sigma}_{AB}} ,$$

with $\bar{\sigma}_{AB} = \frac{1}{N} \sum_{R_A}^{R_B} \sigma_{\Delta R}$ and $N = (R_B - R_A)/\Delta R$.

The spatial resolution allowed by the ratio analysis will be ultimately limited by the bandwidth of the receiver. The transmitter pulse widths must of course be short enough to be compatible with resolution requirements. Field tests[8] carried out with 100 nsec. laser pulses have shown signature distortion, as predicted, since the probe pulse is comparable in width to the return lidar signal. To eliminate errors from this distortion, the laser pulse width should be kept below about 30 nsec.

### 4.2.2 "Slope" Method

The data can also be analyzed by evaluating the so-called "S-function",[5] based on Equation 2-1:

$$S(R) = \ln \frac{R^2 P(R)}{f(R)} + \text{constant} \qquad (4\text{-}3)$$

from which the range-averaged value of atmospheric extinction coefficient $\sigma$ is

$$\bar{\sigma} = -\frac{1}{2} \frac{\Delta S}{\Delta R} . \qquad (4\text{-}4)$$

This method will average out, to a certain extent, inhomogeneities that ordinarily occur in heavy fog. In the case of distinct boundaries in the fog, however, it is necessary to segregate the relatively homogeneous sectors before applying Equation 4-4. For each region, a least squares computation is made to find the average slope.[5]

### 4.2.3 Ratio vs Slope: A Comparison

In contrast to the ratio method, which can be characterized as "microscopic", the slope analysis is a macroscopic approach. Since a least squares fit is used to reduce data to a single average slope, the slope method needs a long baseline $\Delta R$ for adequate representation, and to smooth local inhomogeneities.

On the other hand, the ratio method requires accuracy over a number of small intervals. The smaller the intervals $\Delta R_i$, the more accurate the raw data must be to obtain a given accuracy in the extinction coefficient using ratios.

The ratio method is perhaps the more versatile; not only are details of fog structure available in the data, but almost any subequent computations can be done including the analysis by the slope method. Thus, in a sense, the ratio method includes the other. However, interpreting the detailed data probably requires a digital computer, whereas the slope method, especially when inhomogeneities are not severe, seems well fitted to analog techniques. Analysis in nonuniform fog conditions presents a more formidable task, however, and it remains to be seen if analog techniques can be successfully applied.

## 4.3 ACCURACY

Measurements made with lidar must be accurate enough that derived values of visibility will have legal and operational meaning. For example, if SVR is "measured" as 300 meters, it should not be actually 200 or 400 meters. An accuracy of ten or fifteen percent ($\pm$) is probably sufficient.

Fluctuations, inhomogeneities, and time varying conditions present a different kind of accuracy requirement than do more uniform conditions. In stable, homogeneous fog, accurate readings are possible. In unstable conditions, accuracy requirements are more difficult to define. In such cases--which usually are the most difficult for landing--what is needed is a prediction of the minimum visibility likely to be encountered, along with an indication of the rate and magnitude of prevailing fluctuations.

It is useful to estimate the accuracy with which the lidar system can measure the extinction coefficient, in the absence of disturbing instabilities. In this case, we assume that the uncertainty in measured quantities leads to the major error.

Choosing two values of R beyond the peak of the lidar signal, with measured returns $P_1$ and $P_2$, we find

$$\rho \equiv \frac{P_1}{P_2} = \frac{f(R_1)R_2^2 \, e^{-2\sigma(R_1-R_2)}}{f(R_2)R_1^2} \tag{4-5}$$

and

$$\ell n\rho = \ell n \left[\frac{f(R_1)R_2^2}{f(R_2)R_1^2}\right] + 2\sigma(R_2-R_1). \tag{4-6}$$

Differentiating,

$$\frac{d\rho}{\rho} = 2\Delta R d\sigma = 2\sigma\Delta R \, \frac{d\sigma}{\sigma} \quad , \tag{4-7}$$

with $\Delta R = R_2 - R_1$.

Finally,

$$\frac{d\sigma}{\sigma} = \frac{1}{2\sigma\Delta R}\left[\frac{dP_1}{P_1} - \frac{dP_2}{P_2}\right] \tag{4-8}$$

Some important features of Equation 4-8 are:

- The slope accuracy improves as the interval $\Delta R$ is made larger. (If $\Delta R$ is taken too large, however, the presence of important inhomogeneities may be missed).
- The better the visibility, the larger the percentage error in the measurement of visibility, for given $\Delta R$ and measurement errors dP. (Due to the flatter slope of the lidar signature as visibility improves).
- Uncertainity in P(R) due to random noise can give either positive or negative values for $dP_1$, $dP_2$. However, systematic errors (such as drifting zero levels) would tend to cancel.

- Ultimately, the values of $dP_1$, $dP_2$ depend on the signal-to noise ratio.

## 4.4 APPROACHES TO SIGNAL PROCESSING

Two basic acquisition methods, boxcar (or "slow") and transient recorder ("fast"), have been discussed and compared in Section 3.3. The selection of one method over the other will depend on several factors, including the scale of complexity (and cost) which can be committed to the problem of signal processing. One important consideration will be whether a dedicated minicomputer is to be available for processing and interpretation.

For example, to best exploit the transient recorder, one would strobe, into the buffer register of a minicomputer, the entire body of "words" representing a single lidar backscatter signature; successive signals may be handled similarly or not, depending on the goal one pursues.

If averaging these data for successive signals is desired (and in virtually all situations, averaging will be needed with moderate peak power sources), the computer can do this, provided an interface is available which can handle the data rate. Taking the Biomation recorder as an example, (Section 3.3.2), a compatible interface is available having data transfer rates as high as $2 \times 10^6$ words/sec; this allows direct transfer of data for a lidar pulse repetition rate as high as 1 kHz.

Direct access to a computer is ideal; the decision of how many pulses to average can be made by the computer, adding flexibility to such things as updating intervals. However, computer participation in, and control of, the averaging of transient recordings may be a more elaborate approach than absolutely needed for lidar signal processing.

There are alternatives. For example, recorded data on individual output channels can be averaged with analog circuitry (i.e., RC circuits). This has been done[8] with the Biomation which has both analog and digital outputs, using a waveform eductor with 100 RC channels to read and average successive Biomation recordings.

To so approach the averaging of transient recorder data, however, nullifies the most unique advantage of this device: its applicability to instant analysis. Only if analog averaging is a temporary step in the planned system evolution--the eventual goal being minicomputer control--would the transient recorder have a distinct advantage over slower electronic methods.

# 5. INTERPRETATION OF DATA

## 5.1 NEED FOR INTERPRETATION

To be useful for aircraft landing operations, the processed lidar signal has to be interpreted. The technical and operational phases of the actual SVR measurement routine will need careful management. Data may be in various stages of analysis on reaching the "interpretative" stage. They have at least been recorded in either analog or digital form; perhaps also some analog operations have been performed. The busy pilot or harried controller wants the information reduced to a few simple "statements". The tasks for the system designer are:

1. to survey visibility conditions as they commonly affect landing decisions and
2. to arrive at the most reliable methods for identifying these conditions with lidar and for reporting their presence.

The simplest condition to measure with a lidar (or any other visibility device) is a uniform spatial distribution of aerosols, where a single number characterizes the visibility. Using the slope method of analysis (Section 4.2.1), for example, the data can be reduced to a single slope, whose value gives the extinction coefficient. "Interpretation" includes the conversion from extinction to visibility, a trivial step in this example except for one thing: With respect to the overall "approach volume", uniformity cannot be assumed. It must be shown as part of the "interpretation" process itself. To ignore this need can lead to serious misinformation.

## 5.2 INHOMOGENEOUS ATMOSPHERIC VISIBILITY CONDITIONS

One can appreciate the need for careful interpretation of the lidar data by examining some commonly occurring weather situations. We idealize these situations here to identify characteristic patterns of fog and clouds. Real formations are usually combinations

of these "ideal" forms. In the following, the lidar is assumed to sit in the approach region, near a point on the ground where a pilot would look from decision height.

a. Uniform ground fog:
Decision height above fog layer (Figure 7-a).
The fog layer covers the entire airport as well as the surface of the approach region. It extends from the ground to a height less than the decision height. In this situation, a lidar (L) may be able to sense the top of the layer and also measure the average extinction within the layer. Depending on the height of the layer and its average extinction coefficient, the overall visibility along the critical path (DB) may be good enough to permit landing. Under the same conditions, visibility measured by the RVR transmissometer, if converted to SVR without information about the fog height, might in some cases unduly discourage landings.

b. Uniform ground fog:
Decision height inside layer (Figure 7-b).
Here the visibility along BD is given correctly by either the transmissometer or lidar. The lidar may or may not be able to "see" the top surface; the SVR will be the same in either case.

c. Overcast clouds:

Decision height below clouds (Figure 7-c).
The lidar can act as a ceilometer here, while revealing clear viewing over the critical path BD.

d. Overcast clouds:
Decision height in clouds (Figure 7-d).
In this case, without accurate SVR information, the pilot cannot know what to expect at the decision point. The transmissometer reads clear visibility; yet the pilot may not be able to see the approach lights until he is well below the decision height. Lidar can measure the extinction in the cloud and report SVR.

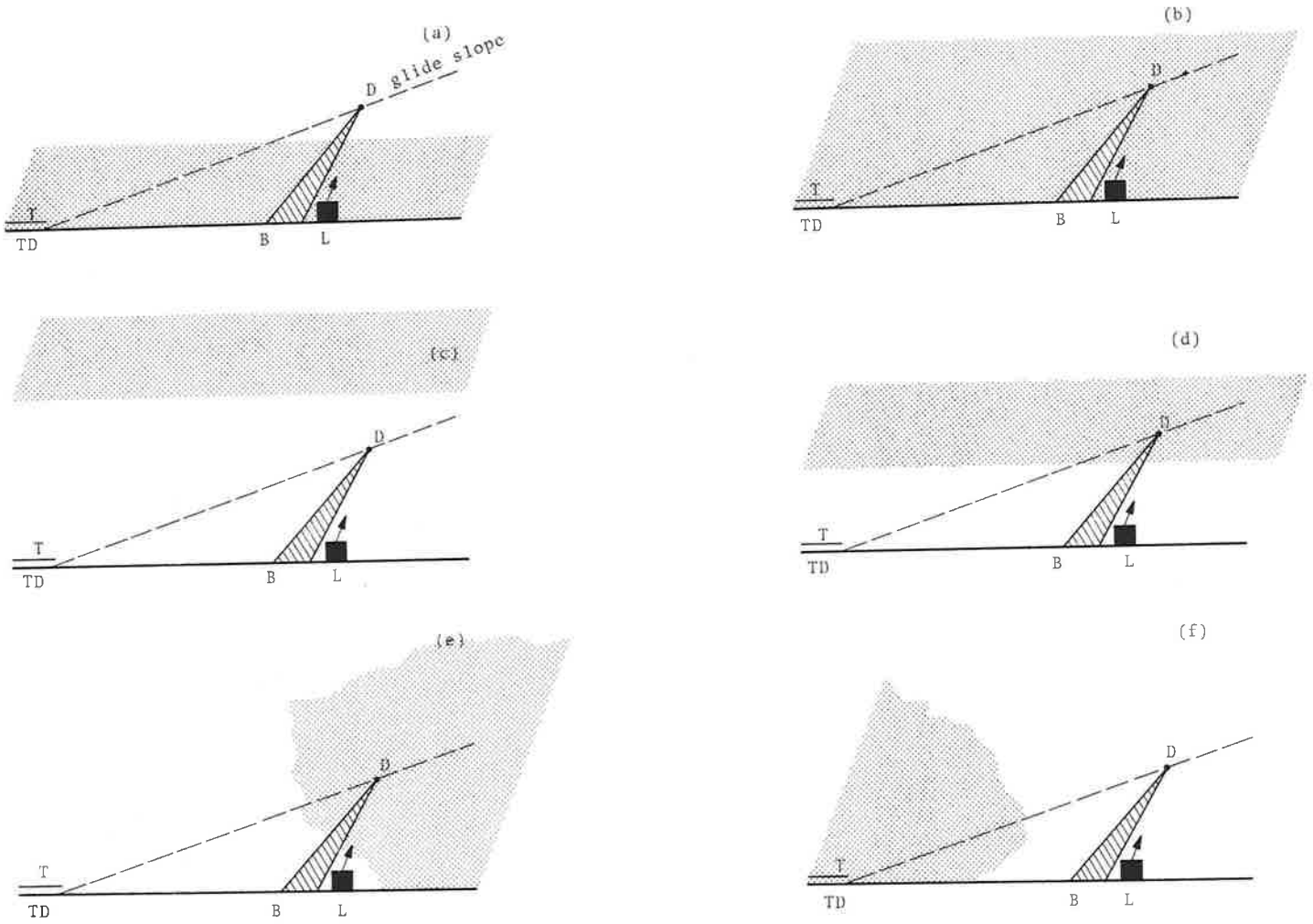


Figure 7. Visibility Patterns Which Can Confront Pilot on Approach Path. Dotted Regions are Fog or Clouds. L, Position of Lidar; T, Transmissometer. $\overline{DB}$, Critical Line of Sight for Pilot at Decision Height D.

e. Fog bank covering approach zone:
Runway clear (Figure 7-e).
Similiar in some ways to case (d), this situation is best handled with a lidar that scans. The lidar itself may be in or out of the bank; if inside, it cannot depict the true situation without scanning. Note that if the lidar is in a clear atmosphere, it can detect a bank of fog as far away as 1 mile.[6]

f. Fog bank covering runway:
Approach region at least partially clear (Figure 7-f).
Here, as long as the fog bottom doesn't rise above the level of the transmissometers (14 feet), the RVR will govern the operations. Notice how by coordinating the transmissometer reading with the lidar result, ambiguity can be reduced in this case and also in case (e).

Among these six patterns, in only two cases (b and c) can the SVR conditions be described as uniform. Yet, the RVR transmissometers would "perceive" each case as if it were uniform. In addition, there are time varying conditions and vertical gradients which add to the task of quantifying visibility. Patchiness and variability at the onset and at the termination of general fog conditions are especially troublesome, while blowing patches of fog, broken low clouds or moving fog banks often accompany poor visibility conditions. The location of an airport largely determines which of the above cases are most common to it.

It is, perhaps, the rare occasion when "visibility" can be represented by a single number. Certainly, in case d and e, one wants spatial resolution of the extinction coefficient. And in most of the remaining cases, a measurement of ceiling and average extinction, at least, is desirable. Finally, the degree of variability, if significant over the duration of an updating interval, needs to be reported.

## 5.3 AUTOMATION

Some degree of automation will be needed to handle the numerous items which enter interpretation. These items contribute in various ways to the overall evaluation of SVR. They include:

- background luminance, as it affects illuminance thresholds
- approach light intensity
- time varying data, useful for predicting trends
- RVR readings
- information obtained from scanning; gradients in structure (particularly vertical).

Of the factors listed, several resemble those encountered in RVR computations (background, light settings). Others are not treated in the RVR case, for two reasons. First, the information reported by the transmissometer is based on a measurement integration, both in space (250 foot baseline) and in time*(approximately one minute); gradients and, to some extent, fluctuations tend to average out. In addition, the present RVR computer has been restricted to basic computations and is not able to perform subsidary calculations which might enhance the information output (e.g., degree of variability, excursions in minimum and maximum RVR, trends).

Lidar on the other hand, as a new tool with potential for spatial resolution, almost begs for more comprehensive interpretation. In view of its promise to provide fine grained input data, lidar calls for a refined analysis. The computation power of a minicomputer is a sine qua non of success in such interpretation.

Two of the above items, bearing on the potential use of lidar, warrant further attention here.

---

* Although transmission data is available at the transmissometer recorder on a time scale of seconds, the reported RVR is based on the one minute average.

### 5.3.1 Time Variations

Variations in backscatter signature with time can occur for several reasons:

1. the average visibility may be slowly changing;
2. the spatial distribution of aerosol density may fluctuate
3. the fog may be moving quickly, causing the average visibility to change rapidly.

An automated SVR system should sense these conditions, and report them properly.

Slow changes: If the average visibility changes slowly and fluctuations are not significant, the analysis and interpretation is not a problem. "Slowly" means at a rate less than the averaging time of the system. Of course, inhomogeneity may still cause difficulty but temporal problems are minimal.

Fluctuations: Fluctuations are of particular concern when they occur at rates comparable to, or slightly less than, updating rates. Perhaps the most critical time in the flight of an aircraft is the last minute or two before landing. In that period, the pilot must have confidence that he will see cues at and below decision height.

Simple indications, such as "go - no go", or "SVR = ____ ft." will be best. More than one or two updating reports in these crucial moments will probably be burdensome. Yet the pilot must be informed of significant variability, both in time and in space, in the SVR status. Accordingly, the system will have to be able to find and evaluate fluctuations and then to reduce this information to simple form, to give the pilot a "sense"of the situation.

A fluctuation is "significant" when it causes the measured visibility category (e.g., II, III) or the indicator message (e.g., go - no go) to change erratically. Such variability is most likely to occur in marginal visibility--the most dangerous

for operations. This fact emphasizes the need to include capability for fluctuation-analysis in the design of both the signal processing and the interpretive subsystems.

Rapidly Changing Conditions: Unstable weather conditions, usually accompanied by winds blowing patches of fog or low clouds, will perhaps provide the most severe test for a lidar system. Not only are these conditions by nature inhomogeneous, but the average extinction along a given sighting segment can change in a time comparable to an updating interval.

Predictions, Trends: Another use for the capabilities of a minicomputer is in the prediction of the short term visibility based on trends in the current data. A weighting scheme may be used to assess the probability of sudden changes and to reduce the operational effects of fluctuations. Similar weighting methods have been proposed for computing RVR from transmissometer measurements.

### 5.3.2 Scanning

A lidar which can scan in a vertical plane offers added coverage and improves the sampling range. One application of scanning, suggested by Collis, et.al.[4], and outlined below, may, under certain circumstances, overcome the lidar's near field inadequacy.

Figure 8, taken from Reference 4 (Figure 16), represents a "height layer" scheme for evaluating the extinction coefficient above the surface. At each elevation angle (including 0°) the lidar signature is analyzed over the darkened segments, to give the average extinction coefficient $\bar{\sigma}_i$ within the ith layer. One assumes that only vertical gradients are significant. The total transmittance T over any slant path (and from it, the visibility along the path) can be found from $T = \exp(-\Sigma\sigma_i l_i)$; $l_i$ is the length of the path segment within layer i.

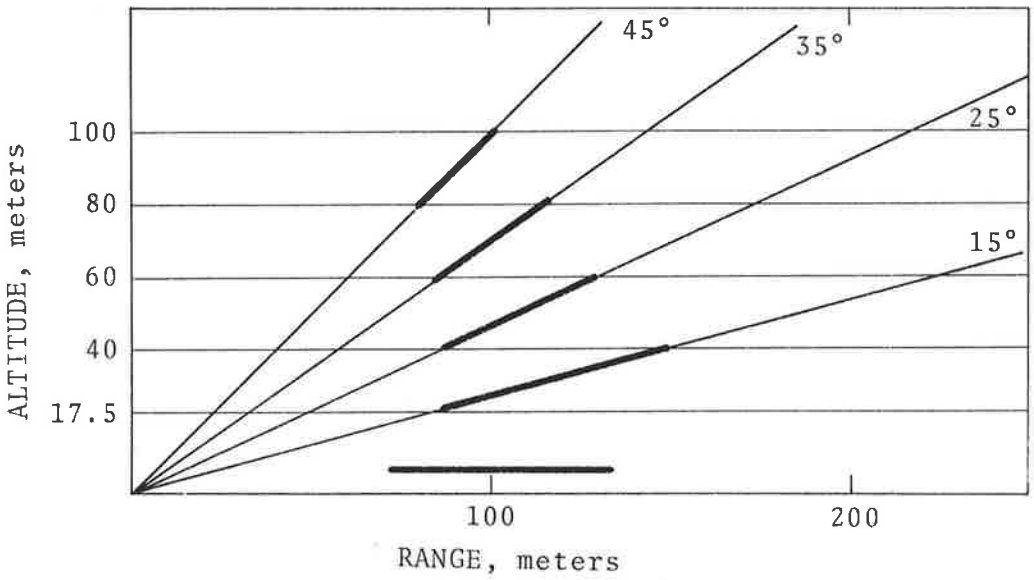


Figure 8. Height Layer Scheme for Evaluation of Extinction Coefficient Above the Surface (from Reference 4)

Collis et al ,[4] claim that their experimental test of this method gave "subjectively satisfying" results. One attraction of this scheme is that the entire critical path can, in principle, be characterized by a combination of measured $\sigma$'s. The loss of information from the first 100 feet or so, due to near field obscuration, etc., would no longer be a problem.

One does not gain such advantages easily, however. Evaluating extinction over given segments, and at several angles of elevation, requires either a longer update interval or a more stringent limit on the system averaging time. Also, mechanical scanning introduces the complication of moving parts, inevitably reducing the reliability of the system and adding to its cost. Finally, scanned data would require a two-dimensional analysis, leading to more sophistication and cost in its processing and interpretation

# 6. CONCLUSIONS

The lidar technique promises to provide a means for monitoring many kinds of low visibility conditions. In particular, the method is unique in its ability to give critical information about visibility along slant paths of interest to pilots on landing approaches.

Still, before lidar can be used operationally, several areas must be confronted which will define the working limits of the system. These include:

* Techniques to handle detector and receiver dynamic range
* Operational implications of minimum and maximum range limits
* Selection of preferred signal processing (instant vs time average)
* Interpretation of data, particularly in inhomogeneous and/or rapidly varying conditions
* Treatment of multiple scattering (see Appendix B)

While some of these topics can be dealt with in the process of hardware design, others (e.g., multiple scattering, data interpretation) will probably require extensive testing of an engineering prototype system to acquire a "feel" for their operational significance.

Furthermore, some fundamental design decisions depend on operational criteria which have not been defined. For instance, the choice between the use of a high peak power, low repetition rate source (e.g., erbium laser,[28] for eye safety) and a high repetition rate but moderate peak power laser source (e.g., gallium arsenide) will depend to some extent on operational criteria. The reason lies in the apparent advantage given by the peak pulse source in situations where low patches of fog are present. Viezee et al.[7] have pointed out that such conditions often both precede and follow the general onset of fog over an area.

Under such circumstances, a high power source may best provide the necessary penetration to discover what lies beyond the early patches. It is perhaps debatable whether a single pulse return every 15 seconds will provide more meaningful data than the average over many pulses in the same period of time; still, this is an example of the need for more detailed operational desiderata.

When evaluating the place of lidar in visibility measurement, one must ask what are the alternatives for measuring slant visibility. With the exception of the FAA-sponsored off-set tower measurements currently being conducted by the Crane Naval Ammunition Depot[10] at NAFEC, there is no other proposed method viable today. And the tower concept, relying as it does on measurements of extinction taken at a 1300 foot offset from the approach zone, is at best an indirect indication of slant visibility along the approach path. The tower method is viewed only as an "interim" solution to the problem of SVR measurement.

This report has tried to present both the possibilities and limitations of lidar visibility instrumentation. On balance, we believe that the technique shows enough promise for useful slant visibility determination that its development should be pursued vigorously.

# APPENDIX A

# EYE SAFETY CONSIDERATIONS

## A.1 LASERS AND EYE SAFETY

Intense highly collimated beams of optical radiation, characteristic of laser sources, can be hazardous to the eye and must be used with care. Any source which is to become the basis for an operational lidar system must be designed to ensure eye safety for all reasonable situations.

The effect of optical radiation on eye tissues has been the subject of many studies; an excellent review of present understanding in the field is given by Sliney and Freasier.[19] There are several physical mechanisms by which radiation can damage ocular components, particularly when very intense nanosecond pulses are involved; thermal damage to the chorioretinal tissue is the most important one to be considered, for the type of laser likely to be used in a lidar.

For a given corneal irradiance $E_c(w\text{-}cm^{-2})$ the amount of radiant energy absorbed in the chorioretinal tissue depends on several things: the size of pupil opening, the entrance angles of the incident light, and the ocular transmission and retinal absorption characteristics for the spectrum of the incident radiation. The temperature rise of the absorbing tissue depends on its specific heat, the retinal image size, and the relative rates at which energy is deposited in and conducted away from the image region.

## A.2 STANDARDS FOR OCULAR EXPOSURE LIMITS

There are several sets of exposure criteria which have been published. Recommended limits for ocular exposure, according to some commonly quoted recent standards, are summarized in Table A-1 (from Reference 19, p. 11).

Values listed as "ANSI Z-136" were proposed in late 1972 by the American National Standards Institute (ANSI) Committee Z-136, and are essentially those put forth at about the same time by the

TABLE A-1. RECOMMENDED LIMITS FOR OCULAR EXPOSURE TO LASER RADIATION (0.4-1.4 μm) for a 7-mm PUPIL (THIS TABLE IS TAKEN FROM SLINEY AND FREASIER, REF. 19)

Intrabeam Viewing of a Collimated Beam

| Organization | Laser wavelengths (nm) | Exposure duration τ * | Corneal radiant exposure ($J\text{-}cm^{-2}$) | Corneal irradiance ($W\text{-}cm^{-2}$) |
|---|---|---|---|---|
| U.S. Depts. of the Army and Navy (February 1969) | 400-1400 | 5-50nsec | $10^{-7}$ | |
| | | Approx. 1msec | $10^{-6}$ | |
| | | Continuous | | $10^{-6}$ |
| ACGIH (1971) | 694.3 | 1nsec to 1μsec | $10^{-7}$ | |
| | 694.3 | 1μsec to 0.1sec | $10^{-6}$ | |
| | 400-750 | >0.1sec | | $10^{-5}$ |
| U.S. Dept. of Labor 29CRF1518.54 (1971) | 632.8 | Incidental(1sec) | | $10^{-3}$ |
| | | Continuous | | $10^{-6}$ |
| U.S. Dept of the Air Force (September 1971) | 400-700 | 10-100nsec | $1.3\times10^{-6}$ | |
| | | 200μsec to 2msec | $10^{-5}$ | |
| | | 2-10msec | | $5\times10^{-3}$ |
| | | 10-500msec | | $2.5\times10^{-3}$ |
| | 1,064 | 10-100nsec | $6\times10^{-6}$ | |
| | | 200μsec to 2msec | $5\times10^{-5}$ | |
| | | 2-10msec | | $2.5\times10^{-2}$ |
| | | 10-500msec | | $1.3\times10^{-2}$ |
| ANSIZ-136 proposed February 1972 | 400-700 | 1nsec to 18μsec | $5\times10^{-7}$ | |
| | | 18μsec to 10sec | $1.8\times10^{-3}.\tau$ | |
| | | 10-$10^4$sec | $10^{-2}$ | |
| | | >$10^4$sec | | $10^{-6}$ |
| | 700-1060 | 1nsec to 18μsec | $5C_1\times10^{-7}$ | |
| | | 18μsec to 10sec | $1.8C_1\times10^{-3}.\tau$ | |
| | | 10-100sec | $C_1\times10^{-2}$ | |
| | 700-800 | 100-[$10^4$/(λ-699nm)]sec | $C_1\times10^{-2}$ | |
| | | >[$10^4$/(λ-699nm)]sec | | $C_1(\lambda-699nm)\times10^{-6}$ |
| | 800-1060 | >100sec | | $C_1\times10^{-4}$ |
| | 1060-1400 | 1nsec to 100μsec | $5\times10^{-6}$ | |
| | | 100μsec to 10sec | $9\times10^{-3}.\tau$ | |
| | | 10-100sec | $5\times10^{-2}$ | |
| | | >100sec | | $5\times10^{-4}$ |

* τ in seconds; C = exp[(λ-700NM)/224]

American Conference of Governmental Industrial Hygienists (ACGIH). According to Sliney and Freasier, other organizations, such as those listed in Table A-1, are expected to adopt these standards for the most part.

There are several qualifications that must be made in interpreting the table for any given source. These include the pulse width and repetition rate, as well as the source radiance and image size which will determine both the hazardous range for momentary accidental exposure and the caution distance for "staring."[19]

A.2.1 Repetitive Pulsing and Cumulative Effects

The safe limit of exposure to a single short pulse of radiation is determined by the amount of energy which can be absorbed in the retina without causing a local temperature rise above the damage threshold. If the thermal effect associated with one pulse is not dissipated before the next pulse is incident, then the degree of overlap must be considered in estimating the damage threshold.

Calculations based on a model which includes the thermal relaxation rate for chorioretinal tissues indicate that no cumulative effects should occur for repetition rates less than 100 Hz (for pulses shorter than about 10 μsec.). However, pulsed argon-ion laser experiments on monkey eyes, using trains of 10 μsec. pulses, at repetition rates from 2 Hz to 10 kHz, show that cumulative effects occur even for pulse rates of a few Hz.[20] Based on these and similar experiments, empirical correction factors can be used to find the threshold limit value of exposure to repetitively pulsed lasers. No theoretical argument has been found to explain these results.[19,20]

Figure A-1 shows the multiplicative correction factor for repetitively pulsed lasers having durations less than $10^{-5}$ sec. The threshold limit value for a single pulse of a pulse train must be multiplied by this factor (Figure A-1 is taken from Reference 19, p. 23). The correction factor for pulse frequencies greater than 1 kHz is 0.06.

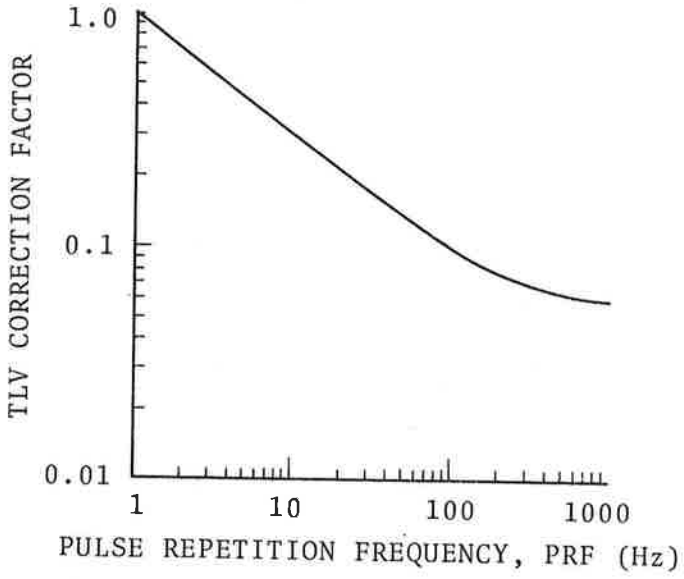


Figure A-1 Threshold Limit Value for Lasers Having $\tau < 10^{-5}$ sec. TLV for a Single Pulse of the Pulse Train is Multiplied by the Above Correction Factor. Correction Factor for PRF Greater than 1 KHz is 0.06. (From Ref. 19)

## A.3 CALCULATIONAL EXAMPLE: GaAs LASER ARRAY SOURCE

We estimate the exposure criteria for a lidar similar to the one described in Table 2-1, presumably with a fiber-optic coupled GaAs array:

$P_o$ = 1 kw ($\lambda$ = 900nm)

$f$ = 1 kHz

$T_p$ = 35 ns

$\theta_{tr}$ = 6 mr (full angle)

$D_o$ = diameter of beam leaving transmitter
= 6 cm (f/1.4)

An observer close to the above transmitter would experience a single pulse radiant exposure $(P_o \cdot T_p)/(\pi D_o^2/4) = 10^{-6}$ J/cm$^2$.

The recommended single-pulse limit for corneal exposure, for a 7 mm pupil (ANSI Z-136) is $5C_1 \times 10^{-7}$ J/cm$^2$, where $C_1 = \exp[(\lambda - 700\text{ nm})/224] = 2.4$. Therefore, the (single pulse) maximum exposure = $1.2 \times 10^{-6}$ J/cm$^2$.

However, the high repetition rate of 1 kHz necessitates a reduction in the single-pulse allowable limit value, by a factor of .06. Therefore, the permissible exposure becomes $7 \times 10^{-8}$ J/cm$^2$.

Consequently, the transmitter with the above characteristics will exceed the permissible exposure limits at the source by a factor of 17. At a distance greater than 30 meters (in clear atmosphere), the safety criterion is met by this transmitter.

By reducing both the output power and repetition rate by a factor of 2, the minimum distance becomes 10 meters. The performance of the lidar would be little affected by such a compromise, as can be seen from Figure 2.

## APPENDIX B

## MULTIPLE SCATTERING

The discussion of the report has assumed that only singly scattered light is received and detected by the lidar. However, with increasing values of optical depth (i.e., $\sigma R$), the probability increases that photons scattered more than once by the aerosol will reach the receiver at the same time as those from single encounters. The geometric paths involved and the consequent constraints on transit time, limit the combinations of events which can contribute to the significant scattering.

For example, the relative amount of double scatter received depends on both the field-of-view of the receiver and on the angular distribution of forward scattered light.[21,22] The latter is a function of $\lambda/r$, where r is the mode radius of the aerosol particles.[23]

Eloranta[21] has given a convenient expression to estimate the double scattering term $P_2(R)$ relative to the single scattering $P_1(R)$ arriving from range R:

$$\frac{P_2}{P_1}(R) \simeq \sqrt{\pi}\ \sigma\ R\ \frac{\delta_{rec}}{\sqrt{<\theta^2>}} \qquad \text{(B-1)}$$

where $\delta_{rec}$ = half angle of receiver field of view

$\theta$ = half angle of forward scattering peak

We can use Equation B-1 to find the expected relative size of double scattering in a typical lidar case. While it is difficult to select a "typical" mean droplet size for fog, we will use $r = 4\mu$. The forward scattering peak then has a half-angle $\theta \simeq 0.1$ rad ($\lambda$ = 800 nm). Let the receiver field of view be $\delta$ = 2 mrad. Then $\delta/\theta \simeq .02$.

The largest optical depth of interest here can be found from the results of Section 2.2, where it is shown that the maximum range $R_m \lesssim V_K$. The optical depth at $R = R_m$ is $\sigma R_m = (3.91/V_K)R_m \simeq 3.91$.

Equation B-1 now yields $P_2/P_1 = .13$. The double scattering is about 10% of the total return and, if ignored, would lead to a 10% error in the measurement of the single scattering amplitude at $R_m$.

Recently, Viezee et al.[7] have found that their lidar-deduced visibility was significantly overestimated, compared to the value measured by a standard transmissometer over the same path. The discrepancy was found to be less than 15% for visibilities between 600 to 1000 feet, but as large as 45% at 300 foot visibility. Viezee et al., have concluded that these discrepancies are predominantly due to multiple scattering additions to the lidar return. However, calculations using Eloranta's expression (Equation B-1) predict an order of magnitude smaller effect. (The field of view used in Viezee et al. was half a milliradian, while the foreward scatter peak half angle was assumed to be 33 mrad. The latter was based on observations of the drop size distribution made at the same time as the lidar measurements.)

At this writing, the above experiment is the only one which has attempted to assess the magnitude of the higher-order scattering in lidar extinction measurements. Clearly, if the discrepancies are as large as implied by the measurements of Reference 7, not only double scattering, but multiple orders of scattering must be considered in any attempt to predict and correct for the effect.

At the present time, there is no way of reliably predicting the contributions of higher-order scattering, though several approaches have been detailed in the literature.[24,25] If indeed the large overpredictions in visibility found by Viezee et al. arise from multiple scattering, empirical methods may be used, as they have shown, to treat these effects. At this point, it is impossible to say how the accuracy will be affected.

## REFERENCES


1. Lomer, L.R., "Fog Detectors for Unmanned Aids to Navigation," U.S. Coast Guard Field Testing and Development Center, Report No. 512 (1970).

2. Schappert, G.T., "Technique for Measuring Visibility," Appl. Opt. 10, 2325 (1971).

3. Brown, R.T., Jr., "Backscatter Signature Studies for Horizontal and Slant Range Visibility," Final Report No. FAA-RD-67-24 (1967).

4. Collis, R.T.H., W. Viezee, E.E. Uthe and J. Oblanas, "Visibility Measurement for Aircraft Landing Operations," Final Report, Contract No. F19628-70-C-0083, Air Force Cambridge Research Labs (1970).

5. Viezee, W., J. Oblanas and R.T.H. Collis, "Slant Range Visibility Measurement for Aircraft Landing Operations." Final Report AFCRL No. 72-0154 (1972).

6. Brown, R.T., Jr., "A New Lidar for Meterorlogical Applications," J. Appl. Meteor. 12, 698 (1973).

7. Viezee, W., J. Oblanas and R.T.H. Collis, "Evaluation of the Lidar Technique of Determining Slant Range Visibility for Aircraft Landing Operations," Final Report (Part II), Contract F19628-71-C-0152 (ADCRL-TR-73-0708) (1973).

8. Lifsitz, J.R., "The Measurement of Atmospheric Visibility with Lidar: TSC Field Test Results," Final Report FAA-RD-74-29, U.S. Department of Transportation (1974).

9. "Slant Visual Range/Approach Light Control Height Measurement Technique with Data Converter and Remote Panel," Engineering Requirement FAA-ER-450-042B (1973).

10. "Slant Visual Range (SVR)/Approach Light Contact Height (ALCH) Measurement System: Evaluation in Fog," Final Report, Phase II, No. FAA-RD-74-7, Department of Defense, Naval Ammunition Deport (1974).

## REFERENCES (CONTINUED)


11. Middleton, W.E.K., Vision Through the Atmosphere, University of Toronto Press, Toronto (1952).

12. Carrier, L.E., G.A. Cato and K.H. von Essen, "The Backscattering and Extinction of Visible and Infrared Radiation by Selected Major Cloud Models," Appl. Opt. 6, 1209 (1967).

13. Pratt, William K., Laser Communication Systems, Wiley, (1969).

14. Schappert, G.T., "Visibility Concepts and Measurement Techniques for Aviation Purposes:" Final Report DOT-TSC-FAA-71-25, Cambridge MA (1971).

15. Lifsitz, J. R., and M.A. Yaffee, "Fog Bank Detector Field Tests: A Technical Summary," Report No. DOT-TSC-USCG-72-2, U.S. Department of Transportation (1971).

16. Oblanas, J.W., W. Viezee and R. Collis, "A Real-Time Lidar Signal Processor," Fifth Conference on Laser Radar Studies of the Atmosphere (1973).

17. Allen, R.J. and W.E. Evans, "Laser Radar (LIDAR) for Mapping Aerosol Structure," Rev. Sci. Instru. 43, 1422 (1972).

18. Rossetto, M. and D. Mauzerall, "A Simple Nanosecond Gate for Side-Window Photomultipliers and Echoes in Such Photomultipliers," Rev. Sci. Instru. 43, 1244 (1972).

19. Sliney, D.H. and B.C. Freasier, "Evaluation of Optical Radiation Hazards," Appl. Opt. 12, 1 (1973).

20. Skeen, C.H., W.R. Bruce, J.H. Tips, Jr., M.G. Smith, and G.G. Garza, "Occular Effects of Repetitive Laser Pulses," Final Report, A.F. Contract "F41690-71-C-0018, Tech, Inc. (1972).

21 Elorant, E.W., "Calculation of Doulby Scattered Lidar Returns," PhD Thesis, Department of Meteorology, University of Wisconsin (1972).

## REFERENCES (CONTINUED)


22. Golubitskii, B.M., T.M. Zhad'ko and M.V. Tantashev, "Influence of Lidar Geometry on the Validity of the Single Scattering Approximation," Izvestia, Atmospheric and Oceanic Physics, 715 (1972) (Translated from the Russian ).

23. Kerker, Milton, The Scattering of Light and other Electromagnetic Radiation, Academic Press (1969).

24. Plass, G.N. and G.W. Kattawar, "Reflection of Light Pulses from Clouds," Appl. Opt. 10, 2304 (1971).

25. Liou, K., "Calculations of Multiple Backscattered Radiation and Depolarization from Water Clouds for a Collimated Pulsed Lidar System," New York University School of Engineering and Science, (1970) (Geophysical Sciences Laboratory Report TR-70-8 ).

26. Klein, N. and T.J. Rock, "A Gated Photomultiplier Technique for Use in Pulse Radiolysis," Rev. Sci. Instr. 41, No. 11, 1671 (1970).

27. DeMartini, R. and K.P. Wacks, "Photomultiplier Gate for Simulated-Spontaneous Light Scattering Discrimination," Rev. Sci. Instru. 38, 866 (1967).

28. Moroz, E.Y., J.P. Segre and N.R. Truscott, "Design and Testing of an Erbium Laser Rangefinder for Use as a Ceilometer," Fifth Conference on Laser Radar Studies of the Atmosphere (1973).